ABSORPTION AND TRANSPORT IN LASER PLASMAS

E. Lindman

ABSORPTION AND TRANSPORT IN LASER PLASMAS

E. L. LINDMAN

Los Alamos Scientific Laboratory P. O. Box 1663 Los Alamos, N. M. 87545, U. S. A.

Résumé. — Les récents travaux expérimentaux et théoriques effectués au Los Alamos Scientific Laboratory sont résumés. Des mesures expérimentales de l'absorption de la lumière laser CO_2, sur des cibles planes, donnent une valeur d'environ 50 %. Des mesures expérimentales des *ions rapides* suggèrent qu'une onde de raréfaction isotherme est un modèle raisonnable pour leur production, et que les estimations précédentes de l'énergie emportée par les ions rapides, étaient trop fortes et erronées. L'absorption résonante avec une forte modification du profil prévoit une forte température électronique, dont les échelles de variation avec la longueur d'onde et l'intensité sont comparables aux valeurs observées expérimentalement. L'instabilité d'ondulation, à laquelle est sujet un saut de densité dans un profil fortement modifié, semble devoir se saturer à amplitude faible. Et finalement, l'inhibition thermique basée sur la résistivité anormale due à la turbulence acoustique ionique ne paraît pas devoir être importante aux densités de solide et au-delà, nécessaires à la fusion par laser.

Abstract. — Recent experimental and theoretical work at Los Alamos Scientific Laboratory is summarized. Experimental measurements of CO_2 laser light absorption on flat targets give a value of approximately 50 %. Experimental measurements of *fast ions* suggest that an isothermal rarefaction wave is a reasonable model for their production, and that previous estimates of the energy carried off by fast ions were erroneously high. Resonant absorption with strong profile modification predicts a hot electron temperature scaling with wavelength and intensity comparable to the experimentally observed values. The rippling instability, to which the density jump in a strongly modified profile is subject, is likely to saturate at low amplitude. And, finally, thermal inhibition based on anomalous resistivity due to ion acoustic turbulence is unlikely to be important at laser fusion densities of solid and above.

Absorption of laser light energy in a plasma and the transport of this energy away from the absorption region are the physical phenomena of most interest to the laser fusion community. Recent work at the Los Alamos Scientific Laboratory has been designed to improve our understanding of these phenomena. The two aspects of laser light absorption which are of interest are : (1) what fraction of the laser light is absorbed ? and (2) in what form is the energy absorbed ? The importance of the fraction of the laser light absorbed is obvious. If a smaller fraction is absorbed more laser light must be provided to accomplish the same thing. The importance of the form in which the energy is absorbed is, perhaps, less obvious. It arises from the fact that the energy transport is affected.

If a certain amount of energy is deposited in all the electrons in a certain region a modest rise in electron temperature occurs. However, if this same amount of energy is deposited in a small fraction of these electrons the energy will be in the form of a few energetic electrons with long mean free paths. These electrons can penetrate the outer materials of a spherically symmetric pellet and preheat the fuel before it is compressed adiabatically. When this fuel is compressed adiabatically to ignition temperature, 3 or 4 keV, the density is lower than it would have been. The number of thermonuclear alpha particles which escapes from the fuel then rises, and the further heating arising from the thermonuclear energy release is reduced. Failure to take advantage of heating from the thermonuclear reaction in this manner is a severe inefficiency.

Energy transport is also affected by other physical phenomena which affect the motion of the hot electrons. Ion sound turbulence is currently being considered as a possible mechanism for inhibiting energy transport below values calculated from binary collisions. Self-generated magnetic fields will also affect the transport, but they are strongly geometry dependent and, hence, difficult to deal with in a general discussion.

It is convenient to divide the recent work at Los Alamos into several topics which have bearing on these considerations.

1. **Absorption of CO_2 laser light on flat targets.** — Vernon Cottles and Damon Giovanielli (LA-UR-77-763) have measured the absorption of CO_2 laser light on flat targets by collecting all the scattered light and comparing it to the incident light. The technique is very similar to that used by van Kessel [1]

et al. for measuring absorption of Nd : glass laser light. The CO_2 laser light is focussed onto a flat target by an off-axis paraboloidal mirror with *f*/2 optics. Some of the scattered or reflected light goes back along the optics. A fraction of it is splitt off and focussed on a calorimeter to measure the fraction of the incident light scattered into the focussing optics. The rest of the scattered light strikes an ellipsoidal mirror which has one of its foci at the position of laser target interaction. All of the scattered light which does not go back through a hole in this mirror into the focussing optics is thus focussed at the second focus of the ellipsoid. A calorimeter placed at this second focus then measures the fraction scattered into the ellipse.

Figure 1 shows the data obtained in this way for an intensity range from 10^{12} W/cm^2 to 3×10^{14} W/cm^2.

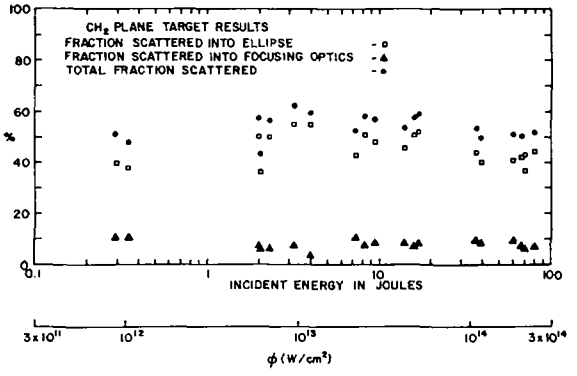

FIG. 1. — Percent of CO_2 laser light scattered into various solid angles vs. energy on target or intensity. The triangles are the percent scattered back into the focussing optics. The squares are the percent scattered into the ellipsoidal mirror. The solid circles correspond to the total scattered light as a percent of the incoming light.

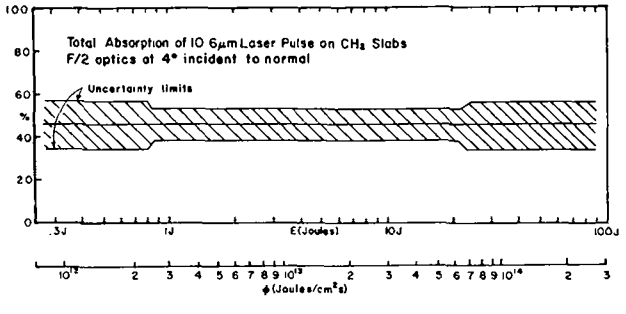

FIG. 2. — Total absorption of CO_2 laser light on CH_2 slabs in the intensity range of 10^{12} to 3×10^{14} W/cm^2. The limits of experimental uncertainty are indicated by the shaded region.

There is typically 5 to 10 % scattered back through the focussing optics and 40 to 50 % scattered into the ellipse. Figure 2 shows the fraction of the incident light absorbed in percent as a function of the incident intensity. The results of this work may be summarized as follows :

1. For the irradiance range of

$$10^{12} \text{ to } 3 \times 10^{14} \text{ W/cm}^2 ,$$

the absorption is a constant 45 $\pm$ 7 %.

2. The absorption is independent of the atomic number (Z) of the material.

3. The scattered light is strongly peaked along the laser-beam, target-normal axis.

4. The azimuthal distribution of the light scattered outside of the focussing optics shows no apparent correlation to the direction of the electric vector of the incident laser light.

2. « **Fast Ions** » **generated by CO_2 laser light on plane targets.** — Fred Young and Gene McCall have recently analyzed the ions generated by CO_2 laser light at an intensity of about 10^{15} W/cm^2 using a Thompson parabola. The ions, deflected into different parabolas depending on their A/Z ratio by parallel electric and magnetic fields were detected by allowing them to impinge on a cellulose nitrate film. After etching with hot NaOH a damage track appears for each ion which strikes the film. Data are obtained by simply counting the holes.

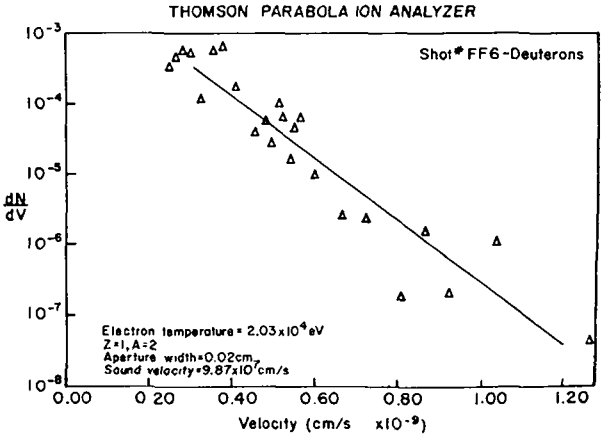

FIG. 3. — Number of deuterium ions as a function of ion velocity from a plane CO_2 target at an intensity of about 10^{15} W/cm^2. The data points are obtained from Thompson parabola analyser, while the solid line is a theoretical fit using a self-similar solution of an isothermal rarefaction wave.

Data obtained in this way for deuterium coming from a CD_2 target are shown in figure 3. The solid line is the number density of ions as a function of ion velocity that is associated with the wellknown isothermal rarefaction wave :

$$n = n_0 \exp\left(-\frac{x + c_s t}{c_s t}\right) = n_0 \exp\left(-\frac{v}{c_s}\right)$$

$$v = c_s + x/t$$

$$c_s^2 = T_e/M_i .$$

The data agree quite well with what one would expect from an isothermal rarefaction wave over four orders of magnitude in density. The structure in the data is real, however, and cannot be ignored.

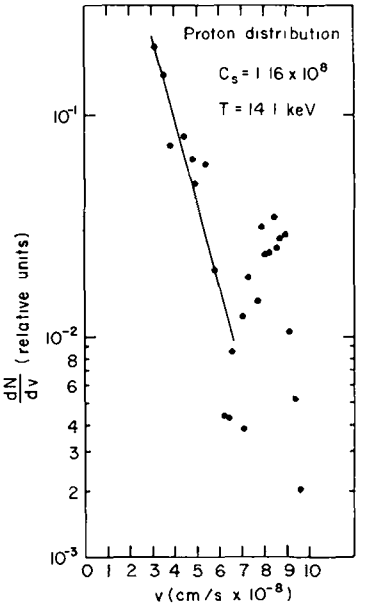

FIG 4. — Number of hydrogen ions as a function of ion velocity from a plane CH_2 target at an intensity of about 10^{15} W/cm^2. Data are from a Thompson parabola analyzer while the straight line is a fit using a self-similar solution of an isothermal rarefaction wave. The deviations from the straight line are probably due to the breakdown of quasi-neutrality as discussed in Ref. [2].

Figure 4 shows similar data for hydrogen coming from a CH_2 target. Again, the isothermal rarefaction wave dependence of ion numbers as a function of velocity is apparent. A new feature is also present, however. There is a local maximum in the ion number at a velocity of 9×10^8 cm/s. This structure has been tentatively identified with a similar structure which occurs in an isothermal rarefaction wave when finite Debye length effects are included. J. E. Crow, P. L. Auer and J. E. Allen [2] have shown that when the spatial scale length of the density is equal to the local Debye length the isothermal rarefaction wave solution breaks down and a maximum velocity for the ions is obtained. The ion distribution in the neighborhood of the maximum velocity shown in reference [2] agrees remarkably well with the data shown here. Of more interest, perhaps, is the structure that appears in the hydrogen data. The Thompson parabola raw data can be used to generate a current trace that would be seen by a charge cup. Such a trace is shown in figure 5. The arrows correspond to an attempt to identify these peaks with charge states $Z = 2$ to 6. This can be done reasonably well in spite of the fact that these are all protons. It is, therefore, suggested that previous attempts [3] to analyze charge-cup traces in this manner were erroneous and the ions thought to be carbon were in fact hydrogen. The fast ion losses are thus substantially less than previously thought.

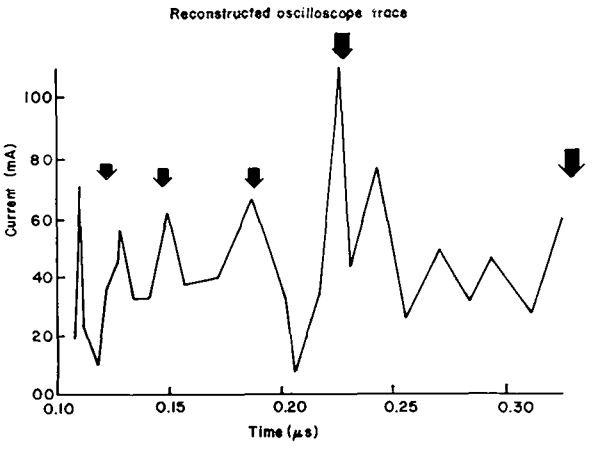

FIG. 5. — Reconstruction of charge-cup current trace using Thompson parabola proton data. The arrows correspond to an attempt to identify peaks associated with the carbon states $Z = 2$ to 6.

3. **Hot electron temperatures from resonant absorption at hight intensity.** — When hot-electron temperatures measured at many laboratories are plotted as a function of intensity for different wavelengths, the curves shown in figure 6 are obtained. The top

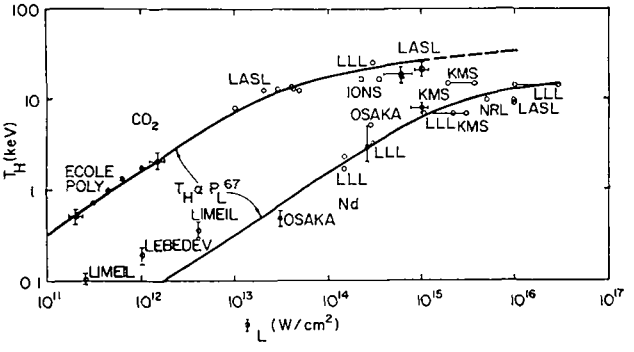

FIG. 6. — Measured hot electron temperature as a function of laser intensity. The two curves correspond to Nd : glass and CO_2.

curve is from Nd : glass experiments while the bottom curve is from CO_2 experiments. These two curves may be combined into one by introducing the parameter, $\Phi\lambda^2$, as shown in figure 7, where Φ is the laser light intensity and λ is the laser wavelength. The physical significance of this parameter lies in the fact that it is proportional to the peak energy attained by an electron oscillating in the electric field of the laser pulse. Two regions in the data are easily distinguished. At high intensities the hot electron temperature is proportional to $(\Phi\lambda^2)^\delta$ where δ is equal to 0.25. At lower intensities a slope, δ, of 0.67 is observed. The high intensity region is the intensity region for

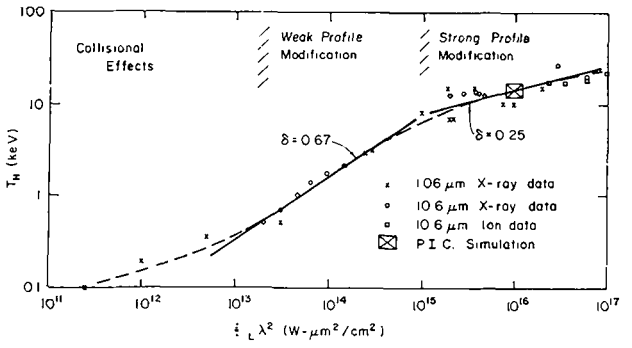

FIG. 7. — Measured hot electron temperature as a function of $\Phi\lambda^2$ (intensity times square of wavelength). The data for the two types of lasers shown in figure 6 fall on the same curve when plotted versus $\Phi\lambda^2$.

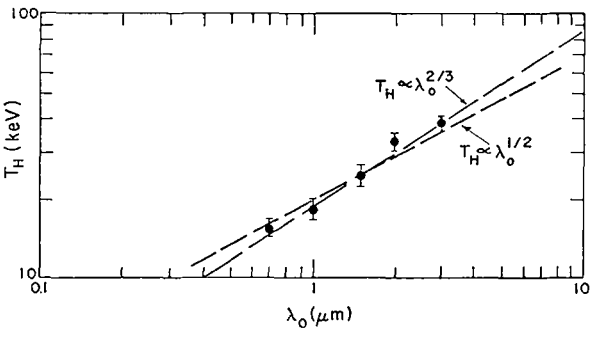

FIG. 8. — Hot-electron temperature as a function of laser wavelength. The data is taken from PIC simulation runs in which the cold electron temperature was held fixed at about 2.5 keV and the intensity was 10^{16} W/cm^2.

laser fusion using CO_2 lasers. It is here that PIC simulation studies of resonant absorption with strong profile modification have been carried out yielding results that agree with the experimental data.

In the early studies of resonant absorption [4] the plasma was initialized with a long gradient length. The electromagnetic wave, which was launched from the left boundary traveling at an angle of about 20° to the x-axis, traveled up the density gradient and was reflected at the classical turning point. Evanescent fields penetrated deeper into the plasma exciting large-amplitude plasma oscillations at the critical surface. These waves were damped by electrons which accelerated out of the plasma oscillation region at high velocity. This system was not in equilibrium, however. Time-average stresses from the large amplitude plasma waves (i. e. the ponderomotive force from the plasma waves) partially evacuated the region in the neighborhood of the critical surface. As time progressed further the flow from the high density region adjacent to the critical surface interacting with the ponderomotive force produced a sharp discontinuity in density from the overdense region to a region of relative constant density well below critical.

It became clear from these simulations that considerable computational expense was going into establishing the equilibrium before the hot-electron temperature of interest could be measured. Since the equilibrium consisted of a sharp discontinuity between a relatively constant density and a very small density, the approach to equilibrium could be sped up by initializing the plasma with a constant density and a vacuum-plasma interface which occurred over several Debye lengths. The electron and ion temperatures are chosen in conjunction with the field amplitude then to give approximate pressure balance.

D. W. Forslund, J. M. Kindel and L. Lee [5] have carried out a number of simulation studies in this manner. Figure 8 shows the hot electron temperature as a function of $\Phi\lambda^2$. From these data it is seen that the hot electron temperature, T_H, satisfies

$$T_H \propto (\Phi\lambda^2)^{0.33} .$$

In figure 9 the hot-electron temperature is plotted as a function of the cold electron temperature, T_c. From these data the following relation is obtained.

$$T_H \propto T_i^{0.33} .$$

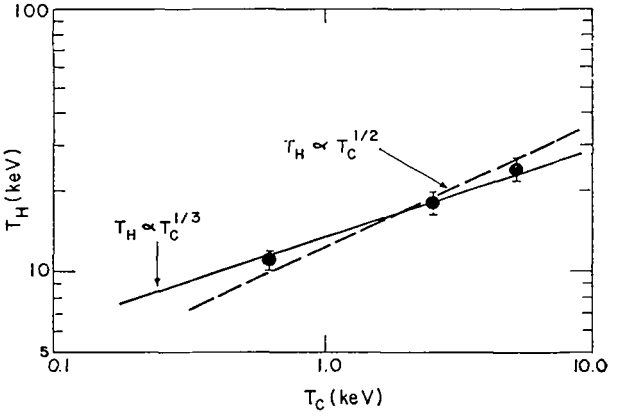

FIG. 9. — Hot electron temperature as a function of T_c, the cold electron temperature. The data are taken from PIC simulation runs in which the intensity was 10^{16} W/cm^2 and the wavelength was 1 μm.

The agreement of the simulation results with the experimental data suggests that resonant absorption may be the dominant absorption mechanism and that strong profile modification may be occurring in the experiments. Furthermore, the weak scaling of the electron temperature with wavelength is very encouraging for the use of CO_2 lasers in laser fusion. Hot-electron temperatures of the order of 10 to 30 keV are expected for CO_2, and these are only a factor of 3 to 5 above those obtained with Nd : glass at these intensities.

4. **Stability of the strongly modified profile.** — Most of the well-known instabilities, which occur in a plasma when an electromagnetic wave is present, are stabilized by the steep gradient. There is, however, an instability that occurs when the plasma pressure is supported by light wave pressure at a sharp inter-

face [6]. It is a rippling or flute type of instability in which the K of the surface perturbation is perpendicular to the electric vector of the incident wave.

PIC simulation studies of this instability have been carried out by D. W. Forslund, J. M. Kindel, K. Lee and E. L. Lindman for the case where the electric field vector is perpendicular to the K of the surface perturbation. Figure 10 shows the nonlinear evolution of the instability. The initial fluting is followed by bubble formation and general destruction of the sharp plasma-vacuum interface.

Two other cases have been run with our PIC simulation code. When the electric field vector is parallel to the K of the surface perturbation no instability is observed. When the electric field vector is at an angle of 45° to the K of the surface perturbation the surface is unstable. The perturbations, however, saturate at low amplitude as shown in figure 11.

We believe the last case is most likely to represent the general case in a 3-dimensional plasma, although the restrictions of a 2-dimensional simulation code prevent complete verification of this conclusion.

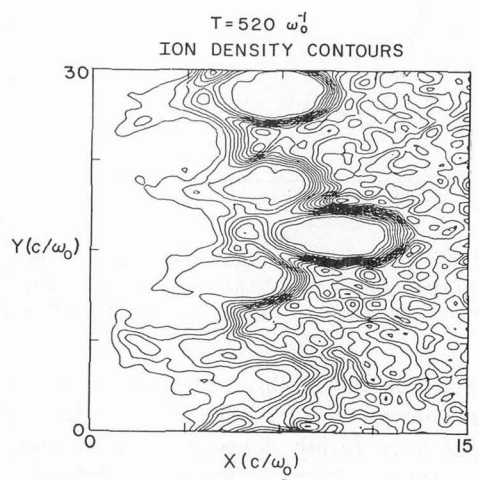

FIG. 10. — Density contours in x-y space from a 2-Dimensional PIC simulation of the surface rippling instability. The light wave is normally incident and its electric field vector is in the z-direction.

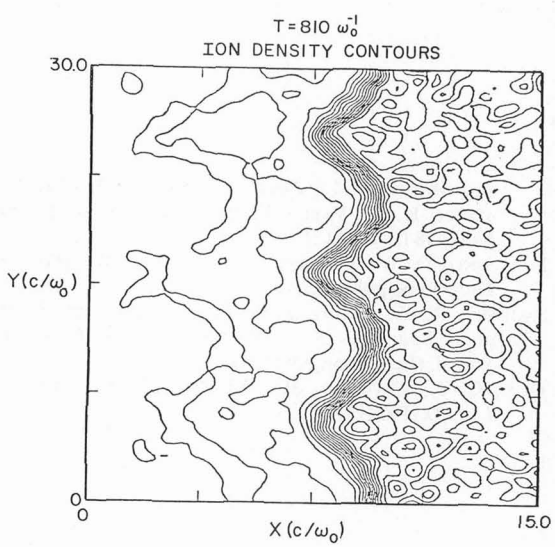

FIG. 11. — Density contours in x-y space from a 2-Dimensional PIC simulation of the surface rippling instability. The light wave is normally incident and its electric field vector is in the y-z plane at an angle of 45° to the z-axis. Saturation at low amplitude is observed for this case.

5. **Ion acoustic turbulence and thermal transport inhibition.** — Two-dimensional PIC studies of thermal transport inhibition and anomalous resistance have been carried out by D. W. Forslund, J. M. Kindel, Ken Lee, E. L. Lindman and R. L. Morse in both the Buneman, or two-stream regime $v_{ed} > v_{eTh}$ and the on-acoustic regime, $v_{ed} < v_{eTh}$. The initial studies of thermal transport inhibition were set up with a combination of hot and cold Maxwellians arranged to give zero current and finite thermal transport. In all cases the drift velocity of the cold Maxwellian with respect to the ions was comparable to or greater than the cold electron thermal velocity. The interaction of the cold Maxwellian with the ions was quite similar to results obtained and published by Dum, Chodura, and Biskamp [7]. The ion acoustic wave turbulence rose quite rapidly and then decayed away. While the turbulence was present a strong anomalous resistance on the cold Maxwellian was observed. The electric field which arose as a result decelerated the hot Maxwellian and reduced the thermal transport substantially. Within a few hundred ω_{pe}^{-1} the turbulence died away, however. The residual resistance on the cold Maxwellian settled down to a value of the order of what one might expect from numerical collisions. The effect of the turbulence was to heat the cold maxwellian to a temperature such that the drift velocity was less than the thermal velocity. The system was thus in the ion acoustic regime, and if there was any anomalous resistance occurring it was inseparable from the effects of numerical collisions. It was concluded that in order to do meaningful simulations in the ion acoustic regime the numerical collision frequency would have to be reduced.

There are two ways to reduce the numerical collision frequency. The first is to use more particles, and the second is to smooth the field. The nature of the first approach is obvious since the collision frequency varies inversely as the particle density in simulation plasmas just as it does in real plasmas. The second approach is most easily described in k space. The simulation is set up so that the lower 20 % of the k values cover the region of instability from which the anomalous resistance will arise. These waves are described quite accurately by the code. Fluctuations at higher k are also present, however. Because too few particles are used, particle correlations lead to field amplitudes substantially above those found in

the problem we wish to simulate. It is reasonable, therefore, to multiply the high k values by a strong reduction factor before Fourier synthesizing the fields and using the fields to update the particle velocities. In practice the smoothing is applied in the form of an operator in x-y space, since a direct method for solving for the potential is used.

Using a combination of these methods simulation studies of thermal transport inhibition was carried out. To maximize the number of particles in the cold Maxwellian, the hot Maxwellian was eliminated. Its role was to supply a current which had to be balanced by the cold return current carried by the cold Maxwellian. The effect of the hot current was retained by requiring $(J_c + \partial E/\partial t)_x = - J_{HX}$. The fact that a sufficient number of particles was used to make the effects of numerical collisions negligible was established in the usual way by doubling the number of particles used and noting that the results did not change.

The simulations were run on a 64 by 64 mesh with physical dimensions of 32 λ_D by 32 λ_D. The drift velocity was typically 0.5 times the electron thermal speed, and 160,000 electrons and ions were used.

The results of these simulations are shown in figure 12. Using mass ratios of 25, 100, 400, and 1 600 a mass-ratio scaling proportional to $(M_e/M_i)^{1/4}$ was obtained. Using electron ion temperature ratios of $T_e/T_i = 50$ and 11, a temperature ratio scaling proportional to T_e/T_i was obtained. From these data the following formula for the anomalous collision frequency is constructed

$$\nu^* = \alpha \frac{T_e}{T_i} \frac{V_{ed}}{V_{e\theta}} \omega_{pe} \left[\frac{m_e}{m_i}\right]^{1/4}$$

$$\alpha = 3 \times 10^{-5} .$$

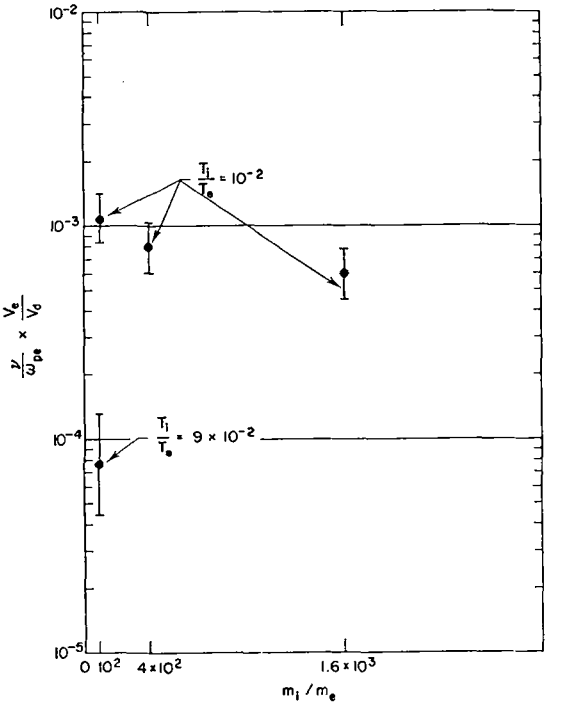

FIG. 12. — Anomalous collision frequency vs. mass ratio. The data are taken from 2-Dimensional PIC simulations of anomalous resistivity due to ion acoustic turbulence.

This anomalous collision frequency is below all of the analytic results currently in the literature. Thus, at laser fusion densities of solid and above, the anomalous thermal-transport inhibition which arises from ion acoustic turbulence is in most cases comparable to the effects of collisions. Furthermore, the ions heat rapidly causing the effect to weaken. It is therefore concluded that ion acoustic turbulence will not have a strong effect on the design of laser fusion pellets.

References

[1] VAN KESSEL, C. G., OLSEN, J. N., SACHSENMAIER, P., SIGEL, R., EIDMANN, K. and GODWIN, R. P., « Diffuse Scattering from Laser Irradiated Plane Targets », 10th European Conference on Laser Interaction with Matter, Ecole Polytechnique, Palaiseau, France (18-22 october 1976).

[2] CROW, J. E., AUER, P. L. and ALLEN, J. E., *J. Plasma Phys.* **14** (1975) 65.

[3] EHLER, A. W., *J. Appl. Phys.* **46** (1975) 2464.

[4] FORSLUND, D. W., KINDEL, J. M., LEE, K., LINDMANN, E. L. and MORSE, R. L., *Phys. Rev.* **A11** (1975) 679 ; ESTABROOK, K. G., VALEO, E. J. and KRUER, W. L., *Phys. Fluids* **18** (1975) 1151.

[5] FORSLUND, D. W., KINDEL, J. M. and LEE, K., *Phys. Rev. Lett.* (to be published).

[6] SAGDEEV, R. Z., *Plasma Phys.* Probl. Controlled Thermonucl. Reactions 3 (1959) 406. *Leontovich*, ed. Eng. Transl. (Pergamon, Oxford).

[7] DUM, C. T., CHODURA, R. and BISKAMP, D., *Phys. Rev. Lett.* **32** (1974) 1231.